JHR 72: 27–43 (2019)
doi: 10.3897/jhr.72.36356
http://jhr.pensoft.net

RESEARCH ARTICLE

JOURNAL OF Hymenoptera RESEARCH
A peer-reviewed open-access journal
The International Society of Hymenopterists

Evolution of glandular structures on the scape of males in the genus *Aphelinus* Dalman (Hymenoptera, Aphelinidae)

Xanthe A. Shirley[1], James B. Woolley[2], Keith R. Hopper[3], Nunzio Isidoro[4], Roberto Romani[5]

1 *USDA-APHIS-PPQ, 2771 F&B Road, College Station, TX 77845, USA* **2** *Department of Entomology, Texas A&M University, College Station, TX 77843, USA* **3** *USDA-ARS-BIIRL, Newark, DE, 19713, USA* **4** *Dipartimento Scienze Agrarie, Alimentari e Ambientali, Università Politecnica Delle Marche, Via Brecce Bianche, Ancona, 60131, Italy* **5** *Dipartimento Scienze Agrarie, Alimentari e Ambientali, Università degli Studi di Perugia, Borgo XX Giugno 74, Perugia, 06121, Italy*

Corresponding author: *James Woolley* (jimwoolley@tamu.edu)

Academic editor: *Petr Jansta* | Received 20 May 2019 | Accepted 6 September 2019 | Published 31 October 2019

http://zoobank.org/BCB88C26-51F8-45F6-B88C-5D2BCDB48578

Citation: Shirley XA, Woolley JB, Hopper KR, Isidoro N, Romani R (2019) Evolution of glandular structures on the scape of males in the genus *Aphelinus* Dalman (Hymenoptera, Aphelinidae). Journal of Hymenoptera Research 72: 27–43. https://doi.org/10.3897/jhr.72.36356

Abstract

The pores and associated glands on male antennae in species of Hymenoptera are involved in mate recognition and are diverse and widespread among taxa. However, nothing has been published about these structures in species of *Aphelinus* (Chalcidoidea: Aphelinidae), a genus of parasitoid wasps with a long history in biological control. Images from scanning electron microscopy (SEM) and transmission electron microscopy (TEM) of *Aphelinus varipes* revealed pores on the ventral side of the male scape that were connected to glands. A survey of the scapes of male antennae in 16 species in six species complexes of *Aphelinus*, as well as two outgroup species, *Aphytis melinus* and *Centrodora* sp., showed that pores were present in all except *Centrodora* sp. The pores varied in several characters: the shape of the structures that carried them, pore size, elevation of the cuticle surrounding the structures, the extent of a carina delimiting the area around the structures, and the number and position of pores. The shape of the pore-bearing structures, the elevation of cuticle around these structures, and the extent of the carina around them map well onto a molecular phylogeny of these *Aphelinus* species. Combinations of pore characters are diagnostic of species complexes, and in some cases, species of *Aphelinus*.

Keywords

Aphelinus, antennal morphology, scanning electron microscopy, scape, sexual dimorphism, mate recognition, glands

Introduction

Successful mating depends on discriminating between individuals of the same versus different species, as well as between potential mates that will yield progeny with high versus low fitness. Communication with pheromones that attract conspecifics and provide cues for their recognition is often a key component in the quest for mates by insects in general and Hymenoptera in particular (for review, see Ayasse et al. 2001). However, more or less elaborate courtship behavior may also be needed to secure mates (for reviews, see Brown 1999, Spieth 1974, Yuval 2006). In parasitic Hymenoptera, courting males often move their antennae in specific patterns and touch females directly with them (for review, see Gordh and DeBach 1978). Such behavior, usually called antennation, often occurs after a male has approached a female, she has stopped walking, and he has climbed on her back so that their bodies are parallel with his head above hers. Starting at this point, males perform various behaviors that may include head-bobbing, antennal waving and stroking, as well as other behaviors, like leg sweeps. Although male antennation during courtship was described at least as early as 1910 (Girault and Sanders 1910), Barrass (1960) in research on *Nasonia vitripennis* (Walker) (Hymenoptera: Pteromalidae) provided perhaps the first quantitative analysis of courtship behavior, which included quantitation of male antennation. In one of a series of papers on reproductive isolation among closely-related species of *Aphytis* Howard (Hymenoptera: Aphelinidae), Rao and Debach (1969) described antennation behavior in Aphelinidae. Gordh and DeBach (1978) later used a quantitative analysis of differences in courtship behavior, including antennation, to distinguish among cryptic species of *Aphytis* in the *lingnanensis* species complex.

The well-documented role of antennation in courtship triggered investigations into the morphology of antennae. Based on scanning electron microscopy (SEM) of antennae, Goodpasture (1975) suggested that the numerous pores on the scapes of males of some species of *Monodontomerus* Westwood (Hymenoptera: Torymidae) might secrete a pheromone. Dahms (1984a) found pores on the ventral surface of male scapes in *Melittobia australica* Girault (Hymenoptera: Eulophidae), for which he had described antennation a decade earlier (Dahms 1973). He proposed that these pores released a pheromone involved in mate recognition, rather than being sensory organs, as had been previously conjectured. This discovery prompted more studies on morphology of male antennae in parasitic Hymenoptera, using SEM and transmission electron microscopy (TEM). Bin et al. (1989) found three types of glands in antennae of *Trissolcus basalis* (Wollaston) (Hymenoptera: Platygastridae), and they suggested roles in courtship and mate recognition. On the ventral side of the fourth antennomere of *Amitus spiniferus* (Brèthes) (Hymenoptera: Platygastridae), Isidoro and Bin (1995) found numerous pores on an elevated plate, and these pores were attached internally to a complex of glandular cells. They suggested that this structure released and spread a mate-recognition pheromone during courtship, and Isidoro et al. (1996) suggested that such structures be called release-and-spread structures (RSS). Research has continued to delineate the taxonomic distribution and morphological diversity of these structures (Bin et al. 1999, Romani et al. 2010).

RSS and their associated glands have been found on male antennae in other chalcidoids: *Trichogramma australicum* Girault (Hymenoptera: Trichogrammatidae) (Amorn-

sak et al. 1998), *Leptomastix dactylopii* Howard, *Rhopus meridionalis* (Ferrière), and *Asitus phragmitis* (Ferrière) (Hymenoptera: Encyrtidae) (Guerrieri et al. 2001). They have also been found in parasitoids in other superfamilies: *Trissolcus basalis* (Wollaston) (Hymenoptera: Platygastridae) (Bin and Vinson 1986), a variety of species of Cynipidae and Figitidae (Cynipoidea) (Isidoro et al. 1999), *Trichopria drosophilae* (Perkins) (Hymenoptera: Diapriidae) (Sacchetti et al. 1999), and *Pimpla turionellae* (Linnaeus) (Hymenoptera: Ichneumonidae) (Bin et al. 1999). In the last two species, the RSS and glands were shown to be necessary for successful courtship and copulation (Bin et al. 1999, Romani et al. 2008).

Observations on courtship behavior in several species of *Aphelinus* Dalman (Hymenoptera: Aphelinidae) showed that males antennate during courtship (Kazmer et al. 1996, Rhoades 2015), but nothing has been published on pores and glands on the antennae of *Aphelinus*. However, antennal pores and glands have been reported on the antennal clubs of males of *Aphytis melinus* DeBach (Romani et al. 1999), which is closely related to *Aphelinus* (Kim and Heraty 2012). Furthermore, observations of slide-mounted *Aphelinus* specimens using differential interference contrast microscopy (DICM) showed that RSS are widespread in the genus, and that the arrangement and shape of RSS differed among species complexes. Here we report results of an investigation of the glandular ultrastructure underlying RSS in scapes of male *Aphelinus varipes* (Förster) using TEM, and a survey of variation in the RSS in 16 species in six species complexes of *Aphelinus* using SEM, DICM, and macrophotography that documents their diversity and shows that they are taxonomically and phylogenetically informative.

Materials and methods

We follow the species complex classification of Hayat (1998), with one modification: we treat the *daucicola* species complex as distinct from the *mali* complex (Hopper et al. 2012).

With TEM, we studied the structure of the cells underlying the pores in the male scape of *A. varipes*. With SEM, we studied male scapes of two to three specimens each from nine species of *Aphelinus* in six species complexes, along with species in two other genera of Aphelininae: *Aphytis melinus* Debach and an undetermined species of *Centrodora* Förster (Hymenoptera: Aphelinidae) (Table 1). With DICM, we studied male scapes of specimens from an additional seven species of *Aphelinus* in two species complexes (Table 1). Prior to preparation for imaging, the material was stored in molecular-grade ethanol.

For TEM, specimens were immersed in a solution of glutaraldehyde (2.5 ml/25 ml solution) and paraformaldehyde (1 g/25 ml solution) in 0.1M cacodylate buffer +5% sucrose, pH 7.2–7.3. The scape was removed from the rest of the antenna and cooled at 4 °C for 3 h. The specimens were placed in 0.1M cacodylate buffer +5% sucrose, pH 7.2–7.3, overnight at 4 °C, then the specimens were post-fixed in 1% OsO4 (osmium tetroxide) for 1 h at 4 °C and rinsed in the previous buffer. Dehydration in a graded ethanol series from 60% to 99% was followed by embedding in Epon-Araldite with propylene oxide as bridging solvent. Thin sections were made with a diamond knife DiATOME ultra 45° (DiATOME AG, Biel, Switzerland) on a LKB Bromma ultramicrotome (LKB®, Sweden), and mounted on formvar-coated, 50-mesh grids. The

sections were stained with uranyl acetate (20 min, room temperature) and lead citrate (5 min, room temperature). Finally, the sections were investigated with a TEM Philips EM 208 (Thermo Fischer Scientific, Hillsboro, Oregon, USA). Digital images with 1376×1032 pixels, 8 bit, uncompressed greyscale in TIFF files were obtained using a high-resolution digital camera MegaViewIII (SIS) connected to the TEM.

For SEM, specimens were critical-point-dried (CPD) using a Tousimis Samdri-790 (Tousimis Research Corporation, Rockville, Maryland, USA), following the manufacturer's protocol. After CPD, two to three males from each accession (Table 1) were mounted onto standard 12.7mm Ted Pella pin stubs using black carbon tape. Specimens were then gold sputter-coated using a Technics Hummer I (Anatech Ltd, Battle Creek, Michigan, USA), following the manufacturer's protocol. Gold was sputtered on specimens for a total of five minutes, in one-minute intervals separated by one minute. All antennomeres on both the left and the right antennae were examined on each specimen. SEM images were acquired using a Tescan Vega 3 microscope (Tescan USA, Warrendale, Pennsylvania, USA) with secondary electron-emission in high vacuum and beam-acceleration voltages ranging from 15 kV to 30 kV. The beam intensity was either 3 or 5 (range is 1–20), and the scan speed was either 6 or 7 (corresponding to 32 or 100 msec/pixel). For DICM, specimens were slide-mounted in Canada balsam using a protocol modified from Noyes (1982) and observed with an Olympus BH2 compound microscope equipped with differential interference contrast and planapochromat objectives. DICM images were captured with a Jenoptik ProGres CT5 digital camera using Image Pro Plus 7.0. Macrophotographic (MP) images were taken of card-mounted specimens using a Macropod Pro setup (https://macroscopicsolutions.com/) consisting of Mitutoyo long-working distance 50× and 100× planapochromat objectives, a Canon 200 mm prime lens, and a Canon EOS 5D Mark III camera. DICM and MP images were focus-stacked using Zerene Stacker 1.04 and final preparation of images from SEM, DICM, and MP was done in Adobe Lightroom. Sample size for specimens examined by DICM and MP varied from a few specimens to ten specimens, or more in cases in which abundant material was available.

Voucher specimens of material examined have been deposited in the Texas A&M University Insect Collection with Voucher #733. Voucher numbers in Table 1 refer to specimens deposited in the Beneficial Insect Introduction Research Laboratory (USDA/ARS), as voucher specimens of the original collections from which colonies were founded.

Five morphological traits of the RSS were recorded for 14 species of *Aphelinus*, as well as for *Aphytis melinus* (Table 2). Eight of these 14 species of *Aphelinus* were studied using SEM, the remainder were studied using DICM. The data were entered into mx, an open-source, web-based database management system (code and documentation available at http://mx.phenomix.org), and the results were also exported as a Nexus file. Diagnostics (Consistency Index and Retention Index) were calculated for each trait using PAUP* with the traits mapped onto a molecular phylogeny from Heraty et al. (2007), modified with additional unpublished data. PAUP* (4.a build 159: Swofford 2002) and the Trace Character History algorithm using the Parsimony Ancestral States in Mesquite (Maddison and Maddison 2018) provided the most parsimonious reconstructions of character state changes on the phylogeny.

Table 1. Collection information and imaging technique for *Aphelinus* species (SEM = scanning electron microscopy, DICM = differential interference contrast microscopy, MP = Macropod macrophotography).

Species complex	Species	Year collected	Country	Host	Host plant	Collector	Permit, voucher	Imaging
subflavescens	*A. perpallidus* Gahan	2009	USA	*Monelliopsis pecanensis*	*Carya illinoinesis*	A. Dickey	TAMUIC voucher 733	SEM
asychis	*A. asychis* Walker	2000	France	*Diuraphis noxia*	*Triticum* sp.	N. Ramualde, D. Coutinot, J. Lopez	P526P-15-04274, AFr00_Dn	SEM
	A. sinensis Shirley & Woolley	2002	China	*Aphis glycines*	*Glycine max*	K. Hoelmer, K. Chen, W. Meikle	P526P-01-53096, AChAg	SEM
abdominalis	*A. abdominalis* (Dahlman)	2014	USA	–	–	Syngenta Bioline	P526P-15-04767, AbUSA_14	SEM
daucicola	*A. daucicola* Kurdjumov	2012	USA	*Aphis helianthi*	*Daucus carota*	C. Dieckhoff	P526P-15-04767, DUSA12_DE	SEM
mali	*A. coreae* Hopper & Woolley	2009	Korea	*Aphis glycines*	*Glycine max*	K. Hoelmer	P526P-08-02142, MKor09_M	SEM
	A. glycinis Hopper & Woolley	2007	China	*Aphis glycines*	*Glycine max*	K. Hoelmer	P526P-01-72318, MCh04_Bj	DICM
	A. rhamni Hopper & Woolley	2005	China	*Aphis glycines*	*Rhamnus* sp.	K. Hoelmer	P526P-01-72318, MCh07_Bj	DICM
	A. mali Haldeman	1985	Australia	*Eriosoma lanigerum*	–	M. Carver, H.J. Banks	ANIC database no. 32 064862	MP
varipes	*A. atriplicis* Kurdjumov	2000	Republic of Georgia	*Diuraphis noxia*	*Triticum* sp.	D. Coutinot	P526P-15-04274, VGg00_Dn	DICM
	A. certus Yasnosh	2001	Japan	*Aphis glycines*	*Glycine max*	R. O'Neil, D. Voegtlin	P526P-01-53096, VJp01_TU	SEM
	near *A. certus*	2009	Korea	*Aphis glycines*	*Glycine max*	K. Hoelmer	P526P-08-02142, VKor09_M	DICM
	A. hordei Kurdjumov	2011	France	*Diuraphis noxia*	*Triticum* sp.	G. Mercadier, M. Roche	P526P-15-04274, VFr11_Dn	DICM
	A. kurdjumovi (Kurdjumov)	2000	Republic of Georgia	*Rhopalosiphum padi*	*Triticum* sp.	D. Coutinot	P526P-13-02503, VGg00_Rp	DICM
	A. nigritus Howard	2015	USA	*Melanaphis sacchari*	*Sorghum bicolor*	–	P526P-15-04767, VUSA14_TX	DICM
	A. varipes (Förster)	2000	France	*Rhopalosiphum padi*	*Triticum* sp.	N. Ramualde, D. Coutinot, J. Lopez	P526P-13-02503, VFr00_Rp	SEM

Table 2. Characters of release and spread structure on male scapes of *Aphelinus* species and *Aphytis melinus*.

Species complex	Species	Pore				Pore region	
		Number	Size[a]	Shape[b]	Location[c]	Carina[d]	Elevation[e]
N.A.	*Aphytis melinus*	2	small	flat	proximal	complete	none
subflavescens	*Aphelinus perpallidus*	2	large	crenulated ridge	proximal	complete	depressed
asychis	*A. asychis*	4	small	flat	midpoint	none	elevated
	A. sinensis	5	small	flat	midpoint	none	elevated
abdominalis	*A. abdominalis*	3	small	cone, round top	distal	complete	depressed
daucicola	*A. daucicola*	5	large	cone, flat top	proximal	complete	depressed
mali	*A. coreae*	2	large	cone, flat top	midpoint	complete	depressed
	A. glycinis	2, 3, 5	large	cone, flat top	midpoint	complete	depressed
	A. rhamni	2, 3	large	cone, flat top	midpoint	complete	depressed
varipes	*A. atriplicis*	3	large	cone, flat top	proximal	half	depressed
	A. certus	3	large	cone, flat top	midpoint	half	depressed
	A. near certus	3	large	cone, flat top	midpoint	half	depressed
	A. hordei	3	large	cone, flat top	midpoint	half	depressed
	A. kurdjumovi	3	large	cone, flat top	midpoint	half	depressed
	A. nigritus	3	large	cone, flat top	midpoint	half	depressed
	A. varipes	3	large	cone, flat top	midpoint	half	depressed

[a] small = diameter of setae base (Fig. 2A–C, E); large, diameter >2× setae base (Figs 2D, 3A–F)

[b] flat = not raised above surrounding cuticle (Fig. 2A, B, E); cone, flat top = on cones, truncated and flat on top (Figs 1A, 3A–F); cone, round top = on cones, rounded on top (Fig. 2C); crenulated ridge (Fig. 2D)

[c] distal = most proximal pore distal to scape midpoint; proximal = most proximal pore proximal to scape midpoint; midpoint = most proximal at scape midpoint

[d] complete = carina completely surrounds pores (Figs 2C–E, 4A); half = at proximal end of pores only (Fig. 4B); no carina around pores (Figs 2A, B, 4C)

[e] none = neither depressed or elevated relative to surrounding cuticle (Fig. 2E); elevated = elevated relative to surrounding cuticle (Fig. 2A, B); depressed = depressed relative to surrounding cuticle (Figs 2C, D, 3A–F)

Results

The male scape in *A. varipes* is characterized by the presence of cuticular modifications located on the ventral side, defining a specialised area (Fig. 1A). The ventral margin presents three subconical elevated areas with truncated and slightly concave tops that carry single pores and which are surrounded by a depressed region delimited by a carina (Fig 1B). In some specimens, a secretion oozing from the pore can be observed accumulating on top of the flattened area (Fig. 1C). Internal observations revealed the presence of a large cell that occupies about half of the whole internal scape volume behind each pore (Fig. 1D). This cell has a large nucleus located in the basal region, a cluster of electron-lucid vesicles located in the middle region, and a straight evacuating duct connected with the external pore (Figs 1D, E). The antennal muscles located within the scape are not connected with the glands, and they are located in the remaining half of the internal scape volume together with the antennal nerve (Fig. 1D, F). Sections taken in a different plane show the presence of a well-developed end apparatus located in the middle region of the cell and characterized by an aporous structure surrounded by microvilli (Fig. 1F, G). Large clumps of electron-lucid vesicles surround the end apparatus (Fig. 1G). The cytological features of the cell are those typical of

intensively active cells, i.e. the presence of a large nucleus and cytoplasm showing the presence of abundant mitochondria and ribosomes (Fig. 1H). The cuticular evacuating duct is connected to the end apparatus and is produced by an associated duct cell with very reduced cytoplasm and a small nucleus (Fig. 1H). The secretion gathered at the level of the end apparatus flows through the evacuating duct and reaches the external pore where it is released.

The morphology of these release-and-spread structures varies among *Aphelinus* species and *Aphytis melinus* (Figs 2, 3; Table 2). The pores in the *asychis* complex are sessile, i.e. not raised above surface of surrounding cuticle, and are on a convex region not surrounded by a carina (Fig. 2A, B). In the other species complexes of *Aphelinus*, the pores are in a depressed region of the cuticle, but individual pores are on elevated structures (Figs 2C, D, 3A–E), which vary from smoothly rounded (Fig. 2C), to crenulated ridges (Fig. 2D), or truncated and volcano-like (Fig. 3A–F). In the two outgroup species, pores are present and sessile in *Aphytis melinus* (Fig. 2E), and absent in *Centrodora* sp. (Fig. 2F).

Mapping six characters of the release-and-spread structures (Table 2) onto a molecular phylogeny of these *Aphelinus* species and *Aphytis melinus* revealed two broad phylogenetic patterns for different sets of characters; one set had shared states for the *mali* and *varipes* complexes and different states in the other species complexes, and the other set had different states in all the species complexes (Fig. 5). For the shape of the structure bearing each pore (Fig. 5A) and the elevation of the region around the pores (Fig. 5C), consistency and retention indexes are 1.0, indicating no homoplasy and potentially useful phylogenetic signal. States for these characters are the same in the *mali* and *varipes* complexes, as well as *Aphelinus daucicola* Kurdjumov, the shape being raised, conical, truncated, and flat or slightly concave on the top with the region around these structures being depressed. The shape varies among the other species, with *Aphelinus abdominalis* (Dalman) having raised structures that are rounded on top, and *Aphelinus perpallidus* Gahan having pores on a crenulate ridge, in both cases surrounded by a depressed region. Species in the *asychis* complex, as well as *Aphytis melinus* have sessile pores, suggesting that sessile pores might be ancestral. However, the surrounding region is elevated in the *asychis* complex, but neither depressed nor elevated in *Aphytis melinus*. Pore size (Fig. 5B) is also the same in the *mali* and *varipes* complexes, as well as *A. daucicola*, and the same in the *asychis* complex, *A. abdominalis* and *Aphytis melinus*, but the consistency index is 0.5 and the retention index is 0.67 because of parallel increase in pore size in *A. perpallidus* and in the lineage consisting of *A. daucicola* through *Aphelinus certus* Yasnosh. For the carina around the pores (Fig. 5D), the consistency and retention indexes are 1.0, indicating no homoplasy and strong phylogenetic signal. However, the state of the carina differs between the *varipes* complex and *mali* complex. Species in the *varipes* complex have a carina around the proximal end of the pores, whereas species in the *mali* complex, as well as *A. daucicola*, *A. perpallidus*, and *Aphytis melinus* have a carina completely surrounding the pores, suggesting that a complete carina is ancestral in *Aphelinus*, although it is absent in the *asychis* complex. Both the number (Fig. 5E) and location of pores (Fig. 5F) have consistency and retention indexes less than 1 (0.6 and 0.5 for pore number; 0.4 and 0.25 for pore location), indicating a fair amount of

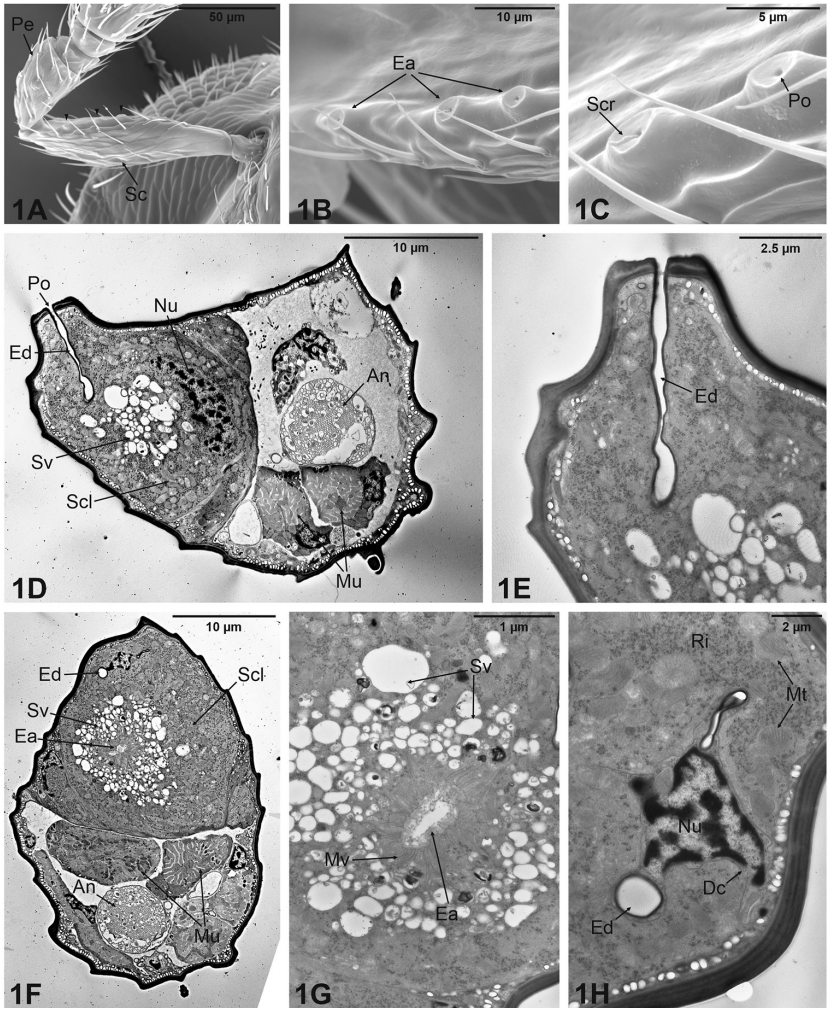

Figure 1. Structure of the male scape in *Aphelinus varipes*. **A–C** Scanning electron microscope images showing in **A** the modified male scape (Sc) with the presence of a ventral carina on which three specialized structures (arrowheads) are observed **B** detail of the carina revealing three elevated areas (Ea) **C** close up of the previous in which a single apical pore (Po) per Ea is clearly visible, as well as secretion (Scr) oozing from the pore itself. **D–H** Transmission electron microscope images showing internal ultrastructural features of the male scape **D** cross section of the scape taken through one of the elevated areas, showing the secretory cell (Scl) that occupies about half of the scape internal volume; Scl has a large nucleus (Nu) located basally, a central cluster of electron-lucid secretory vesicles (Sv) and a straight evacuating duct (Ed) connected with the external pore (Po); the rest of the scape volume is occupied by muscles (Mu) and the antennal nerve (An) **E** close-up view of the previous image, showing the cuticular evacuating duct (Ed) running straight towards the external pore **F** cross section of the scape taken in a different view, showing the large secretory cell (Scl) with a centrally positioned end apparatus (Ea) surrounded by numerous secretory vesicles (Sv); the evacuating duct (Ed), muscles (Mu), and antennal nerve (An) can be seen **G** detail of the end apparatus (Ea), which appears perforated and surrounded by microvilli (Mv); secretory vesicles (Sv) are above **H** detail of the duct cell (Dc) characterised by a very reduced cytoplasm and a small nucleus (Nu); the duct cell is surrounded by the cytoplasm of the secretory cell, that reveals the presence of ribosomes (Ri) and mitochondria (Mt); the evacuating duct (Ed) is visible in cross section. Scale bars: 50 µm (**A**); 10 µm (**B, D, F**); 5 µm (**C**); 2.5 µm (**E**); 1 µm (**G**); 2 µm (**H**).

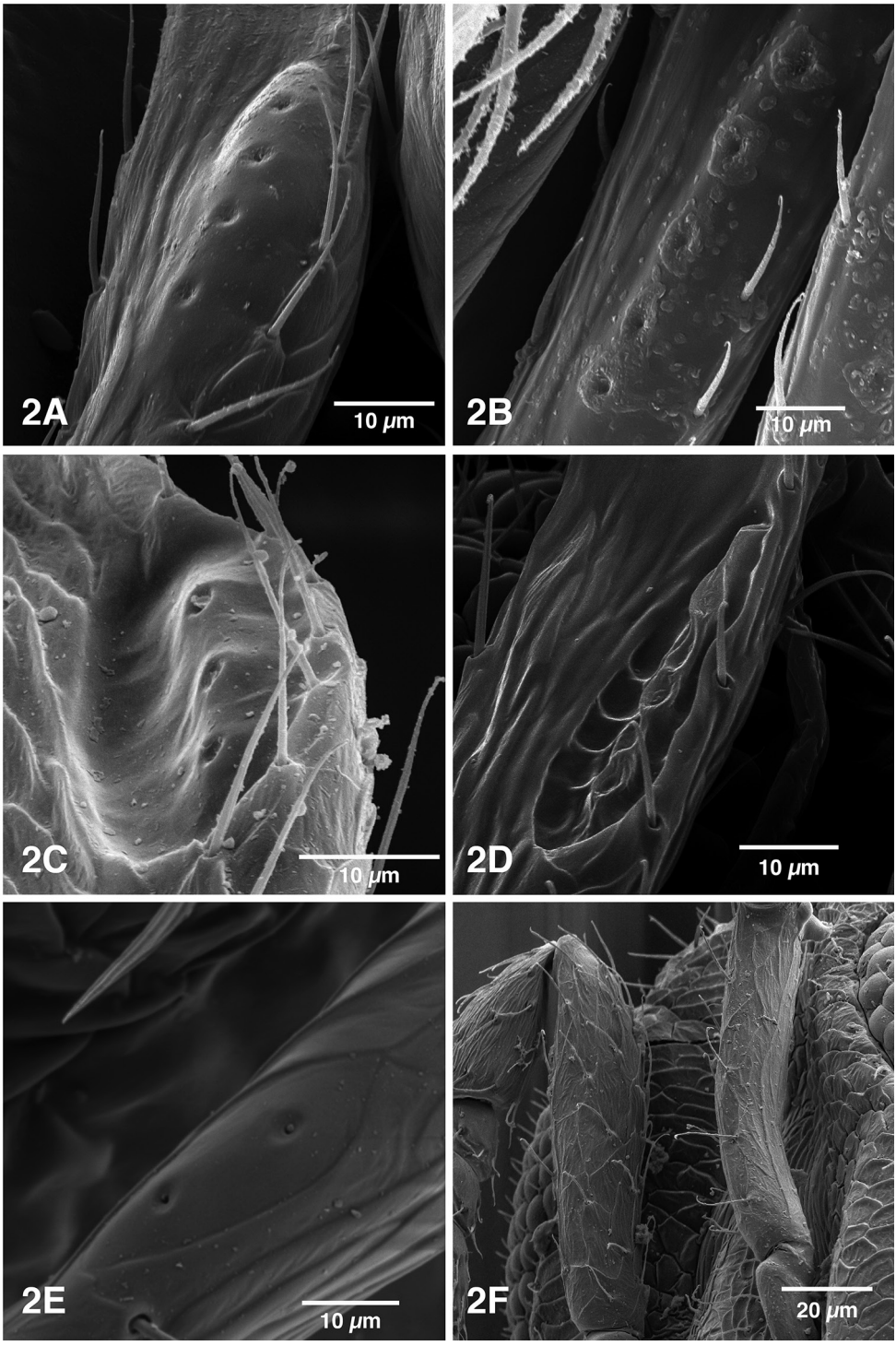

Figure 2. Scanning electron microscope images of the ventral surfaces of male scapes in four *Aphelinus* species and two outgroup species. **A** *A. asychis* **B** *A. sinensis* **C** *A. abdominalis* **D** *A. perpallidus* **E** *Aphytis melinus* **F** *Centrodora* sp.

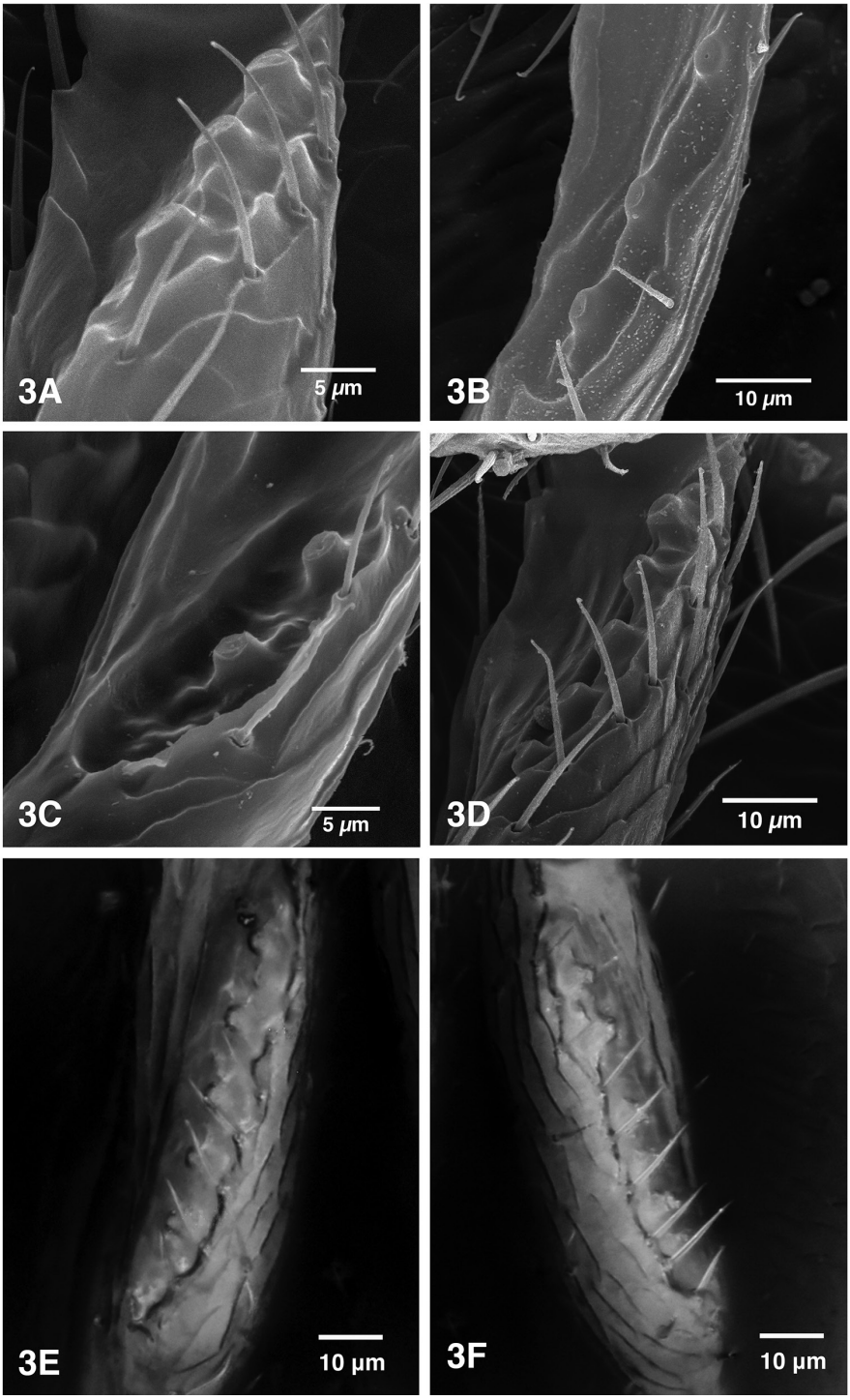

Figure 3. Scanning electron microscope (**A, B, C, D**) and macrophotographic (**E,F**) images of the ventral surfaces of male scapes in five *Aphelinus* species. **A** *A. albipodus* **B** *A. varipes* **C** *A. coreae* **D** *A. daucicola* **E, F** *A. mali.*

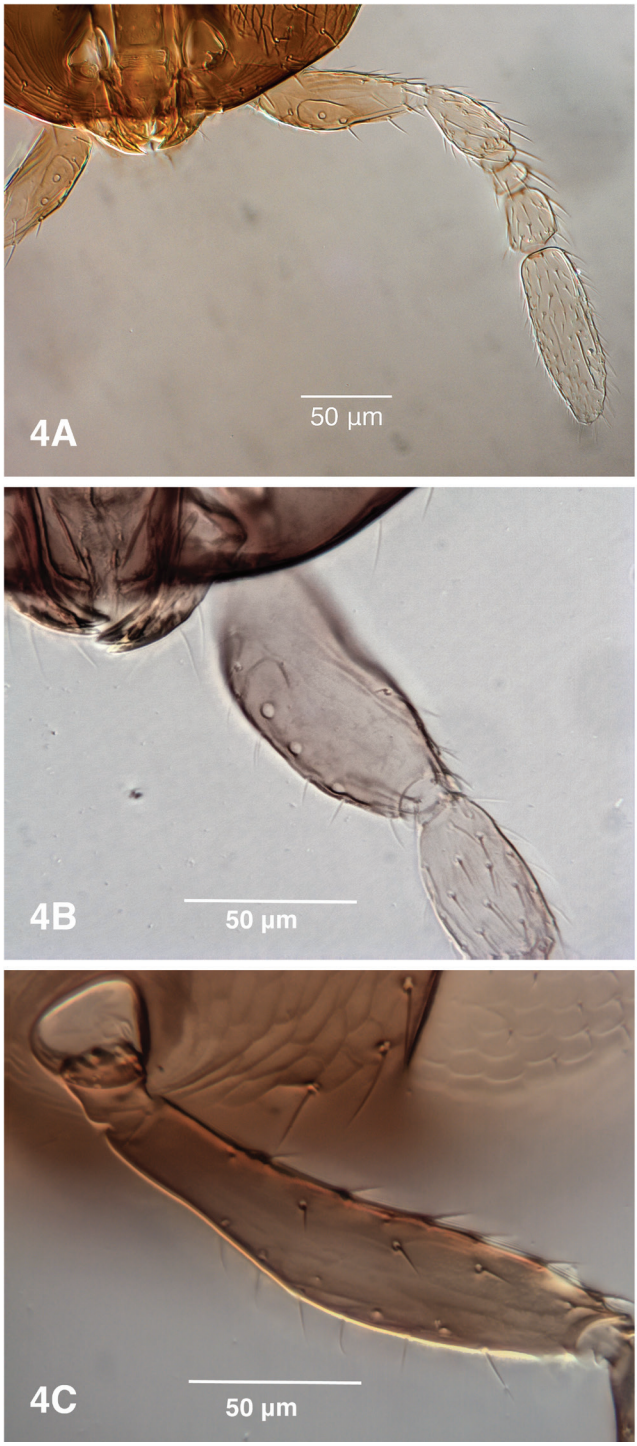

Figure 4. Three states of character representing form of carina on *Aphelinus* male scapes, lateroventral view. **A** Pores completely surrounded by carina **B** carina at proximal end of pores only **C** no carina around pores.

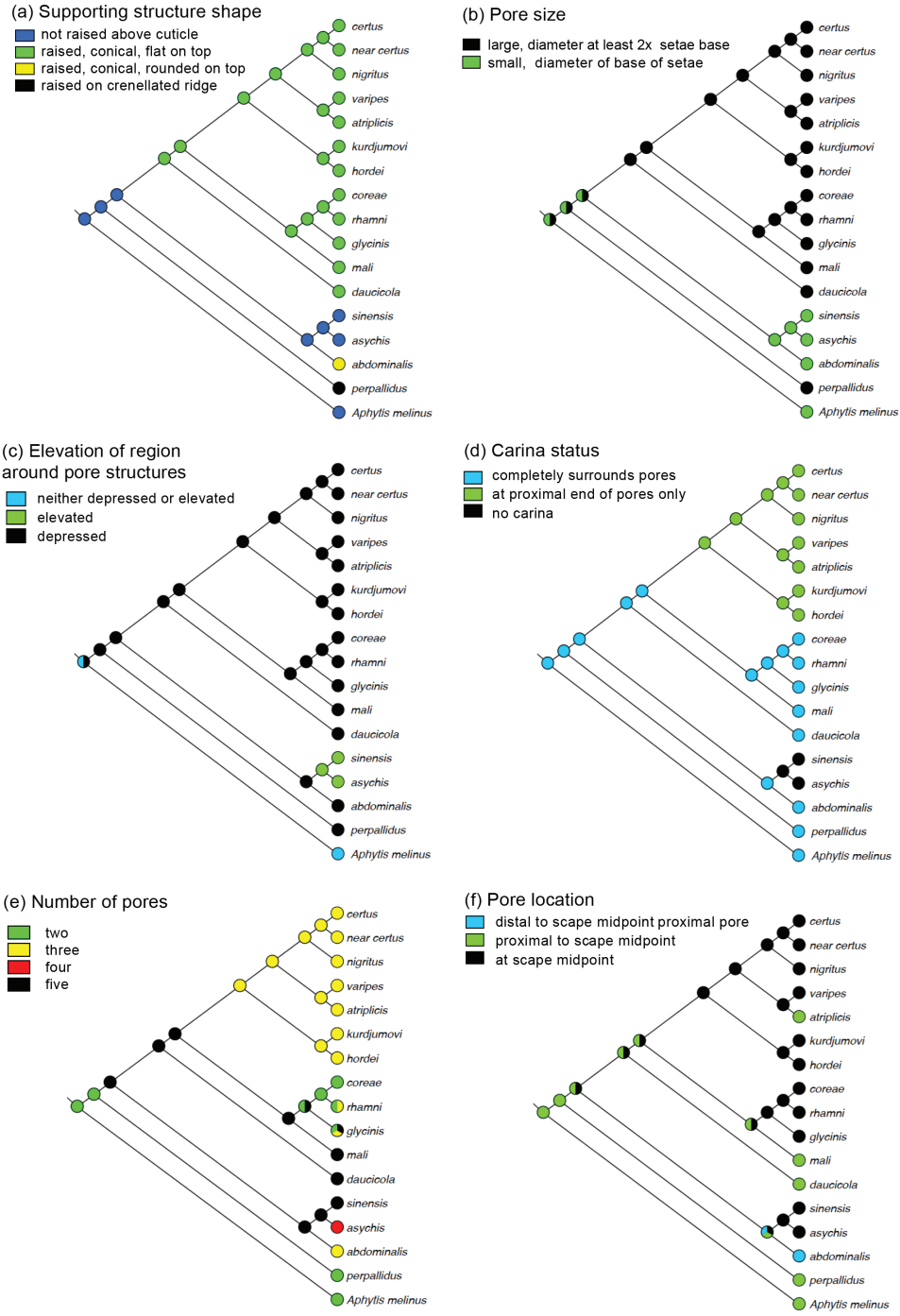

Figure 5. Characters of release-and-spread structures mapped onto molecular phylogeny of *Aphelinus* plus *Aphytis melinus*. **A** Supporting structure shape **B** pore size **C** elevation of region around pore structures **D** carina status **E** number of pores **F** pore location.

homoplasy for these characters. The *varipes* complex is consistent in pore number with all species having three pores. Nine species in the *varipes* and *mali* complexes have the most proximal pore at the scape midpoint. However, *Aphelinus atriplicis* Kurdjumov, *Aphelinus mali* (Haldeman), and *A. daucicola*, have the most proximal pore proximal to the scape midpoint. For *A. mali* and *A. daucicola* this may have arisen because they both have five pores, which might force the most proximal pore further towards the head. Species in the *asychis* complex have four or five pores, but like most species in the *varipes* and *mali* complexes, the most proximal pore is at the scape midpoint. However, species in the *asychis* complex have small, sessile pores that are close together, which may allow them to fit more distally than found in *A. mali* and *A. daucicola*. On the other hand, both *A. perpallidus* and *Aphytis melinus* have only two pores but have the most proximal pore proximal to the scape midpoint, suggesting that fit to the available length may be not be important for pore placement.

Discussion

There is considerable variation among *Aphelinus* species in the characters of the release-and-spread structures on male scapes. Although three characters show some homoplasy with CI values of 0.50 to 0.75 (pore number, size, and location), three characters have CI = 1.0 (supporting structure, elevation of cuticle, and extent of carina). Combinations of characters are diagnostic for species complexes of *Aphelinus* (Table 2), and some combinations are diagnostic for species within complexes. Furthermore, the morphologically distinctive aspects of the male scape in these *Aphelinus* species mapped reasonably well onto the molecular phylogeny. It is intriguing that pores were found on the male scapes of one outgroup taxon, *Aphytis melinus*, but were absent from the male scapes of *Centrodora* sp. Along with *Aphelinus*, both outgroups are members of Aphelininae, but *Aphytis* and *Centrodora* are in the subtribe Aphytini (Hayat 1998) and are closely related members of a clade separate from the lineage containing *Aphelinus* in the morphological phylogeny of Kim and Heraty (2012). A different RSS structure on the antennal club (terminal antennomere) of *Aphytis* males may also play a role in male antennation during courtship (Romani et al. 1999). A broader survey of RSS structures on male antennae in Aphelinidae would be worthwhile.

Aphelinus varipes males have specialized secretory structures on the scape, which are connected with the external pores. The glandular units have secretory cells releasing secretions in electron-lucid vesicles. These vesicles surround an end apparatus connected with the cuticular evacuating duct (produced by a duct cell) that allows the external release of the secretion. These features are typical of secretory cells belonging to class III, according to the classification of insect epidermal glands proposed by Noirot and Quennedey (1974, 1991) and Quennedey (1998). Male antennal glands in this class have been reported for other groups of Hymenoptera, including Symphyta and Aculeata (Bin and Vinson 1986, Bin et al. 1999, Isidoro et al. 1999, Romani et al. 2005, Romani et al. 2008), and functionally, these structures have been related in most cases with courtship behavior by males.

However, despite the numerous cases reported, occurrence of male antennal glands on the scape is relatively uncommon. Dahms (1984a) described the presence of antennal glands on the profoundly modified scape of males of *Melittobia australica*, which are related to stereotyped antennal movements during courtship involving the scape itself.

Dahms (1984b) used differences among structures on the ventral area of male scapes in a revision of the genus *Melittobia* Westwood (Hymenoptera: Eulophidae). Dahms compared his work on *Melittobia* with that of van den Assem et al. (1982) on *Melittobia* and noted that both antennation and morphology of the structures on male scapes varied among *Melittobia* species groups. The species group that did not have extensively modified structures did not antennate as strongly in its courtship as the species groups that had more modified male scapes.

In Aphelinidae, male antennal glands have been reported in *Encarsia asterobemisiae* Viggiani and Mazzone (Hymenoptera: Aphelinidae), *Encarsia aurantii* (Howard) and *Encarsia opulenta* (Silvestri) (Pedata and Isidoro 1993), however, in these species RSS are located on the flagellar segments, not the scape. The functional significance of RSS on the scapes of *Aphelinus* and *Aphytis* (and perhaps other Aphelinidae) presents an intriguing problem in functional morphology associated with mate recognition. By demonstrating the diversity in forms of RSS and by placing this diversity in a phylogenetic context, our results are a first step in unraveling this puzzle. Knowledge of these structures may help in understanding mate selection in this genus, as well as adding to the knowledge about sex glands in parasitic Hymenoptera in general.

Acknowledgements

We thank Andreas Holzenburg and Mike Pendleton of Texas A&M Microscopy Center for assistance with SEM imaging. Thanks to Kim Carr, Texas A&M, for the preliminary male scape survey. Thanks also to Jewel Coffey, Bryant McDowell, and Itzel Cetina, Texas A&M, for help with specimen preparation. We thank Petr Jansta and Ovidiu Popovici for their excellent comments and suggestions for the manuscript. TEM and SEM images of *A. varipes* and SEM images of *A. varipes* were done at the Centro Universitario di Microscopia Elettronica (CUME; Università degli Studi di Perugia, Italy). This research was supported by the following grants from the National Science Foundation, USA: DEB 1257601 and DEB 1555790, and it was part of the M.S. thesis of XAS at Texas A&M University.

References

Amornsak W, Cribb B, Gordh G (1998) External morphology of antennal sensilla of *Trichogramma australicum* Girault (Hymenoptera: Trichogrammatidae). International Journal of Insect Morphology and Embryology 27: 67–82. https://doi.org/10.1016/S0020-7322(98)00003-8

Ayasse M, Paxton RJ, Tengö J (2001) Mating behavior and chemical communication in the order Hymenoptera. Annual Review of Entomology 46: 31–78. https://doi.org/10.1146/annurev.ento.46.1.31

Barrass R (1960) The courtship behaviour of *Mormoniella vitripennis* Walk. (Hymenoptera, Pteromalidae). Behaviour 15: 185–209. https://doi.org/10.1163/156853960X00223

Bin F, Colazza S, Isidoro N, Solinas M, Vinson SB (1989) Antennal chemosensilla and glands, and their possible meaning in the reproductive behavior of *Trissolcus basalis* (Woll.) (Hym.: Scelionidae). Entomologica 24: 33–97.

Bin F, Nunzio I, Romani R (1999) Antennal structures of Hymenoptera: sensilla or glands? Accademia Nazionale Italiana di Entomologia XLVII: 251–263.

Bin F, Vinson SB (1986) Morphology of the antennal sex-gland in male *Trissolcus basalis* (Woll.) (Hymenoptera: Scelionidae), an egg parasitoid of the green stink bug, *Nezara viridula* (Hemiptera : Pentatomidae). International Journal of Insect Morphology and Embryology 15: 129–138. https://doi.org/10.1016/0020-7322(86)90052-8

Bin F, Wackers F, Romani R, Isidoro N (1999) Tyloids in *Pimpla turionellae* (L.) are release structures of male antennal glands involved in courtship behaviour (Hymenoptera: Ichneumonidae). International Journal of Insect Morphology and Embryology 28: 61–68. https://doi.org/10.1016/S0020-7322(99)00015-X

Brown WD (1999) Mate choice in tree crickets and their kin. Annual Review of Entomology 44: 371–396. https://doi.org/10.1146/annurev.ento.44.1.371

Dahms E (1973) Courtship behaviour of *Melittobia australica* Girault, 1912, (Hymenoptera: Eulophidae). Memoirs of the Queensland Museum 16: 411–414.

Dahms E (1984a) An interpretation of the structure and function of the antennal sense organs of *Melittobia australica* (Hymenoptera: Eulophidae) with the discovery of a large dermal gland in the male scape. Memoirs of the Queensland Museum 21: 361–377.

Dahms E (1984b) Revision of the genus *Melittobia* (Chalcidoidea: Eulophidae) with the description of seven new species. Memoirs of the Queensland Museum 21: 271–336.

Girault AA, Sanders GE (1910) The chalcidoid parasites of the common house or typhoid fly (*Musca domestica* Linn.) and its allies. Psyche (London) 17: 9–28. https://doi.org/10.1155/1910/17925

Goodpasture C (1975) Comparative courtship behavior and karyology in *Monodontomerus* (Hymenoptera: Torymidae). Annals of the Entomological Society of America 68: 391–397. https://doi.org/10.1093/aesa/68.3.391

Gordh G, DeBach P (1978) Courtship behavior in the *Aphytis lingnanensis* group, its potential usefulness in taxonomy, and a review of sexual behavior in the parasitic Hymenoptera (Chalcidoidea: Aphelinidae). Hilgardia 46: 37–75. https://doi.org/10.3733/hilg.v46n02p037

Guerrieri E, Pedata PA, Romani R, Isidoro N, Bin F (2001) Functional anatomy of male antennal glands in three species of Encyrtidae (Hymenoptera : Chalcidoidea). Journal of Natural History 35: 41–54. https://doi.org/10.1080/002229301447880

Hayat M (1998) Aphelinidae of India (Hymenoptera: Chalcidoidea): a taxonomic revision. Memoirs on Entomology, International 13: 432 pp.

Hopper KR, Woolley JB, Hoelmer K, Wu K, Qiao G, Lee S (2012) An identification key to species in the *mali* complex of *Aphelinus* (Hymenoptera, Chalcidoidea) with descriptions of

three new species. Journal of Hymenoptera Research 26: 73–96. https://doi.org/10.3897/jhr.26.2584

Isidoro N, Bin F (1995) Male antennal gland of *Amitus spiniferus* (Brethes) (Hymenoptera: Platygastridae), likely involved in courtship behavior. International Journal of Insect Morphology and Embryology 24: 365–373. https://doi.org/10.1016/0020-7322(95)00014-U

Isidoro N, Bin F, Colazza S, Vinson S (1996) Morphology of antennal gustatory sensilla and glands in some parasitoid Hymenoptera with hypothesis on their role in sex and host recognition. Journal of Hymenoptera Research 5: 206–239.

Isidoro N, Bin F, Romani R, Pujade-Villar J, Ros-Farre P (1999) Diversity and function of male antennal glands in Cynipoidea (Hymenoptera). Zoologica Scripta 28: 165–174. https://doi.org/10.1046/j.1463-6409.1999.00013.x

Kazmer DJ, Maiden K, Ramualde N, Coutinot D, Hopper KR (1996) Reproductive compatibility, mating behavior, and random amplified polymorphic DNA variability in some *Aphelinus asychis* (Hymenoptera: Aphelinidae) derived from the Old World. Annals of the Entomological Society of America 89: 212–220. https://doi.org/10.1093/aesa/89.2.212

Kim JW, Heraty J (2012) A phylogenetic analysis of the genera of Aphelininae (Hymenoptera: Aphelinidae), with a generic key and descriptions of new taxa. Systematic Entomology 37: 497–549. https://doi.org/10.1111/j.1365-3113.2012.00625.x

Maddison WP, Maddison DR (2018) Mesquite: a modular system for evolutionary analysis. Version 3.5. http://mesquiteproject.org

Noirot C, Quennedey A (1974) Fine-structure of insect epidermal glands. Annual Review of Entomology 19: 61–80. https://doi.org/10.1146/annurev.en.19.010174.000425

Noirot C, Quennedey A (1991) Glands, gland-cells, glandular units – some comments on terminology and classification. Annales de la Société entomologique de France 27: 123–128.

Pedata P, Isidoro N (1993) Evidence of male sex glands on the antenna of *Encarsia asterobemisiae* Viggiani et Mazzone (Hymenoptera: Aphelinidae). Bollettino del Laboratorio di Entomologia Agraria Filippo Silvestri, Portici 50: 271–280.

Quennedey A (1998) Insect epidermal gland cells: ultrastructure and morphogenesis. In: Harrison FW, Locke M (Eds) Microscopic Anatomy of Invertebrates. Wiley-Liss, New York, 177–207.

Rao SV, Debach P (1969) Experimental studies on hybridization and sexual isolation between some *Aphytis* species (Hymenoptera – Aphelinidae). 1. Experimental hybridization and an interpretation of evolutionary relationships among species. Hilgardia 39: 515–553. https://doi.org/10.3733/hilg.v39n19p515

Rhoades JH (2015) A comparative study of courtship behaviors across the genus *Aphelinus* (Aphelinidae, Hymenoptera). University of Delaware (Newark).

Romani R, Isidoro N, Bin F (1999) Further evidence of male antennal glands in Aphelinidae: the case of *Aphytis melinus* DeBach (Hymenoptera: Aphelinidae). Journal of Hymenoptera Research 8: 109–155.

Romani R, Isidoro N, Bin F (2010) Antennal structures used in communication by egg parasitoids. In: Consoli FL, Parra JRP, Zucchi RA (Eds) Egg Parasitoids in Agroecosystems with Emphasis on *Trichogramma*. Springer Netherlands, Dordrecht: 57–96. https://doi.org/10.1007/978-1-4020-9110-0_3

Romani R, Isidoro N, Riolo P, Bin F, Fortunato A, Turillazzi S, Beani L (2005) A new role for antennation in paper wasps (Hymenoptera, Vespidae): antennal courtship and sex dimorphic glands in antennomeres. Insectes Sociaux 52: 96–102. https://doi.org/10.1007/s00040-004-0780-y

Romani R, Rosi MC, Isidoro N, Bin F (2008) The role of the antennae during courtship behaviour in the parasitic wasp *Trichopria drosophilae*. Journal of Experimental Biology 211: 2486–2491. https://doi.org/10.1242/jeb.013177

Sacchetti P, Belcari A, Romani R, Isidoro N, Bin F (1999) External morphology and ultrastructure of male antennal glands in two diapriids (Hymenoptera: Diapriidae). Entomol Problems 30: 63–71.

Spieth HT (1974) Courtship behavior in *Drosophila*. Annual Review of Entomology 19: 385–405. https://doi.org/10.1146/annurev.en.19.010174.002125

Swofford DL (2002) PAUP*. Phylogenetic Analysis Using Parsimony (*and Other Methods). Version 4. Sinauer Associates, Sunderland, Massachusetts.

van den Assem J, Den Bosch HI, Prooy E (1982) *Melittobia* courtship behaviour: a comparative study of the evolution of a display. Netherlands Journal of Zoology 32: 427–471. https://doi.org/10.1163/002829682X00184

Yuval B (2006) Mating systems of blood-feeding flies. Annual Review of Entomology 51: 413–440. https://doi.org/10.1146/annurev.ento.51.110104.151058